

Supporting Information Figures

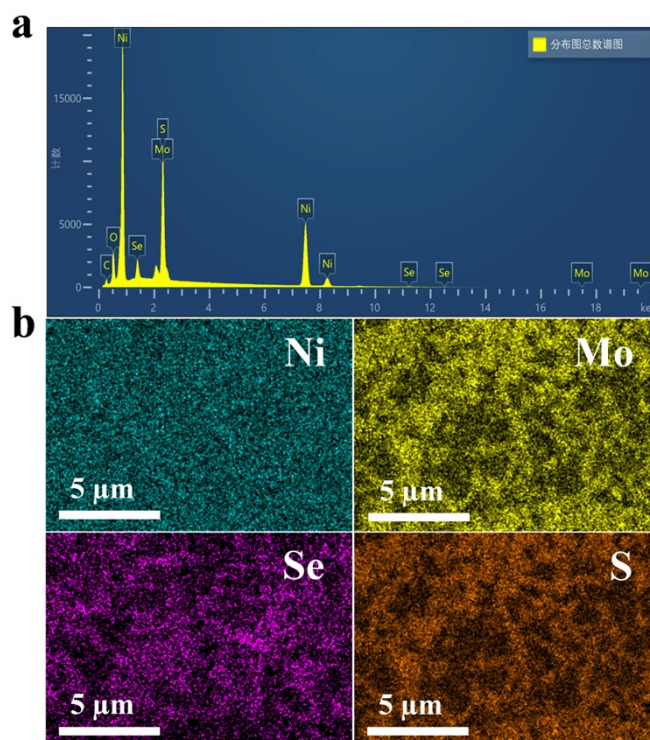


Fig. S1 (a) Contents of each element and (b) Elemental mapping images of S/NiMoSe.

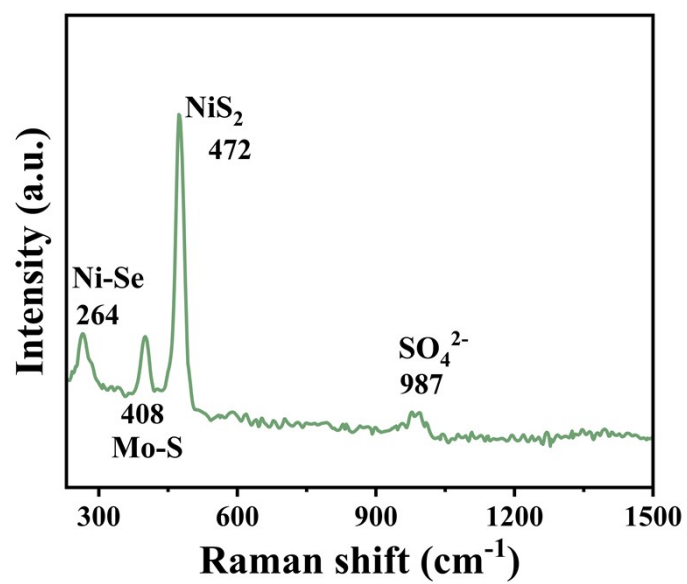


Fig. S2 Raman spectra of S/NiMoSe.

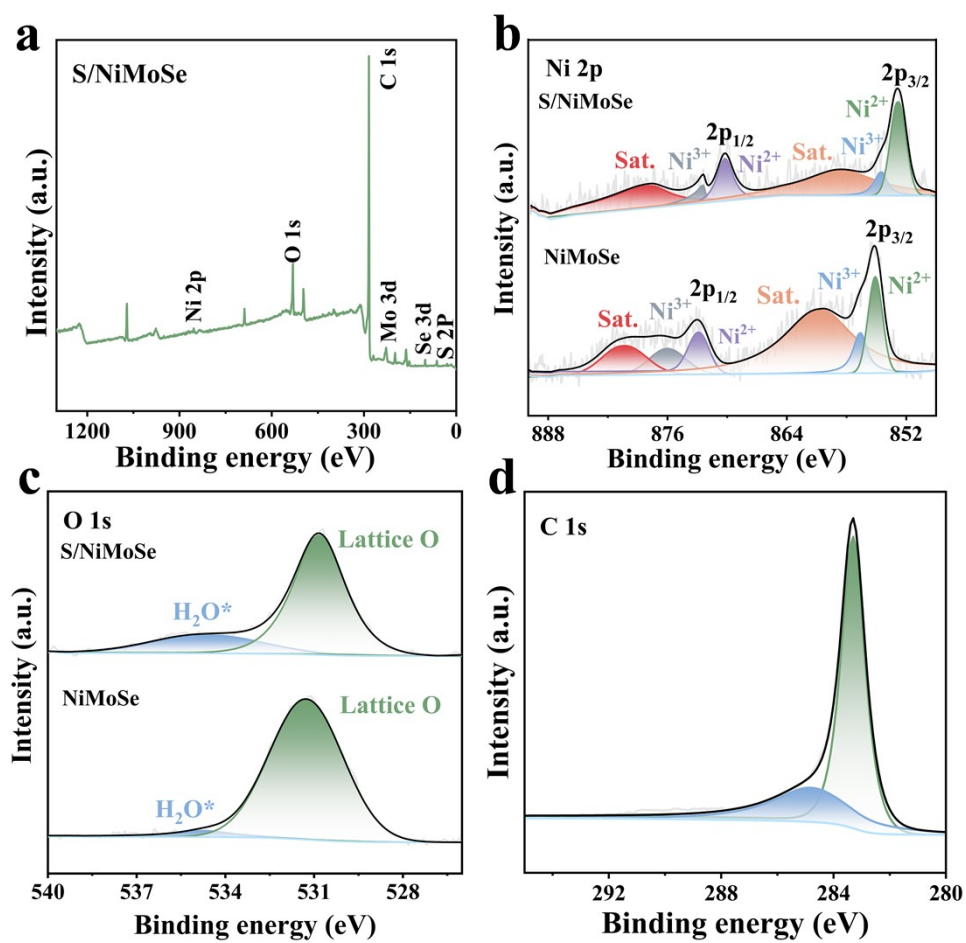


Fig. S3 (a) XPS survey spectra of S/NiMoSe; XPS spectra of (b) Ni 2p and (c) O 1s for S/NiMoSe and NiMoSe; (d) High-resolution spectrum of C 1s for S/NiMoSe.

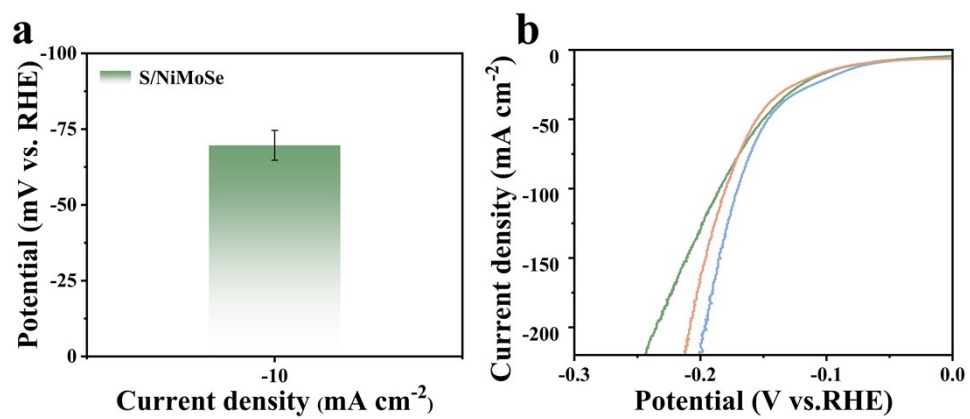


Fig. S4 (a) Error bars for S/NiMoSe represent the standard deviation of overpotentials at a current density of -10 mA cm^{-2} from three parallel tests, with a value of (-69 ± 4.9) mV, and (b) LSV curves of S/NiMoSe obtained from the three parallel test.

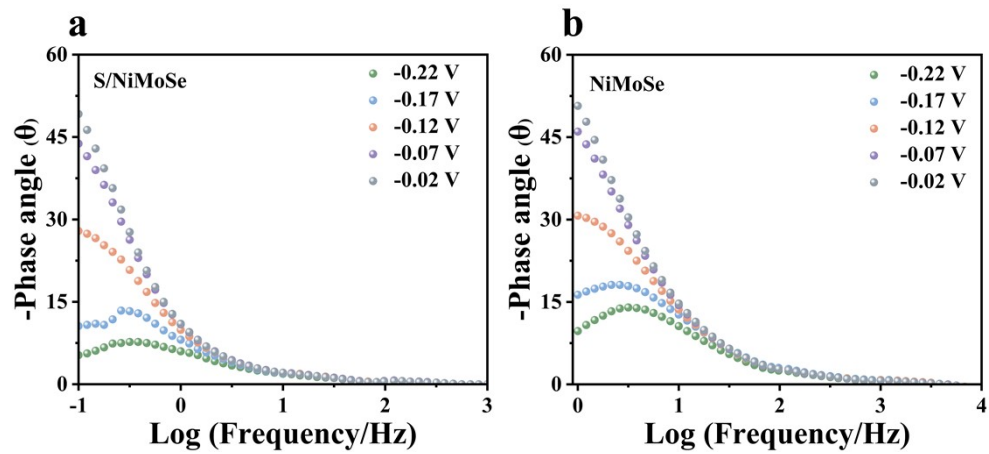


Fig. S5 Bode plots of (a) S/NiMoSe and (b) NiMoSe.

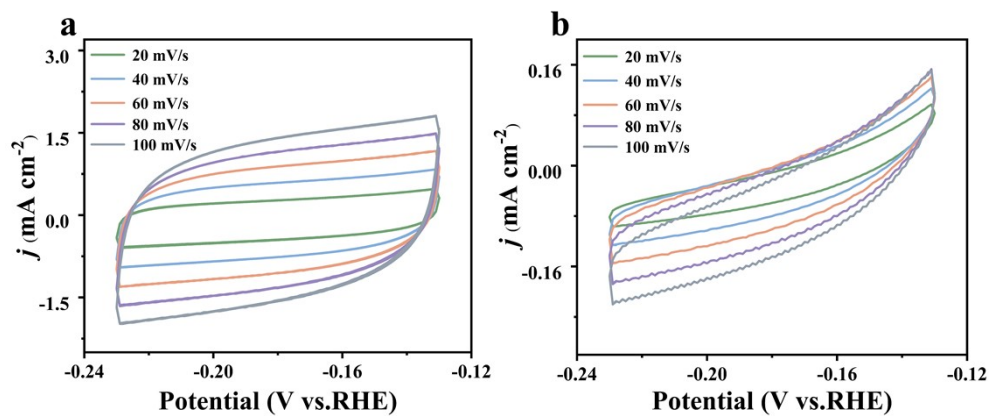


Fig. S6 CV curves at different scan rates for (a) S/NiMoSe, and (b) NiMoSe.

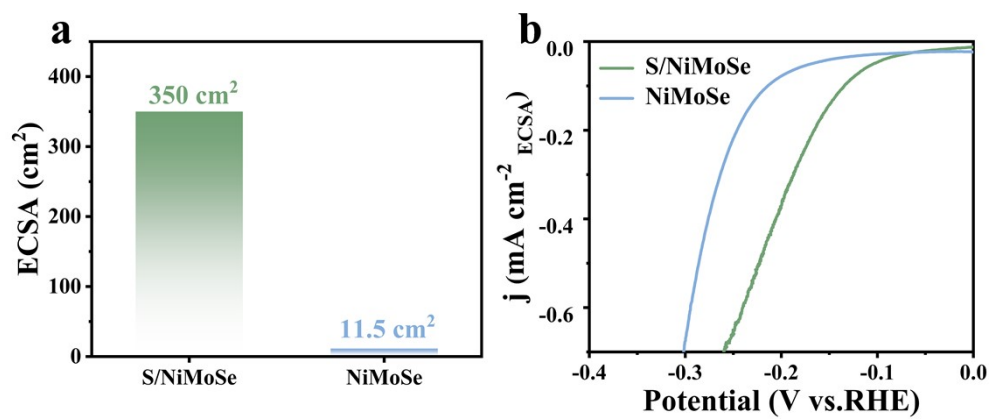


Fig. S7 (a) ECSA values and (b) ECSA-normalized LSV curves of S/NiMoSe and NiMoSe.

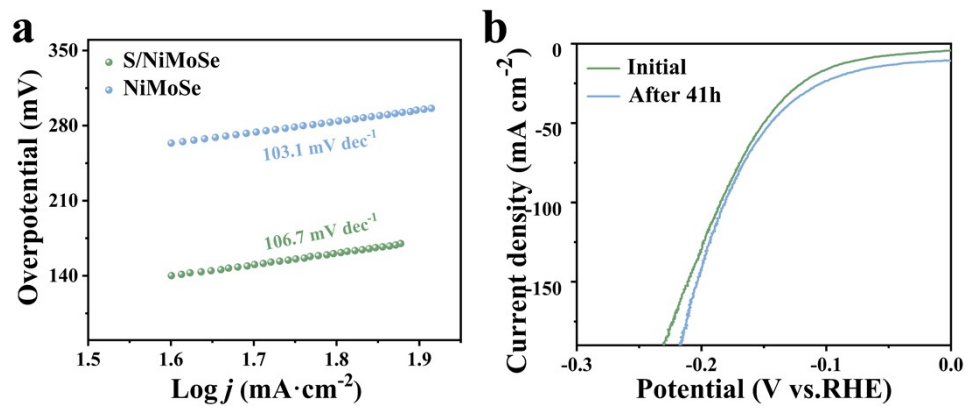


Fig. S8 (a) Tafel slopes; (b) LSV curves recorded before and after the 41 h stability test.

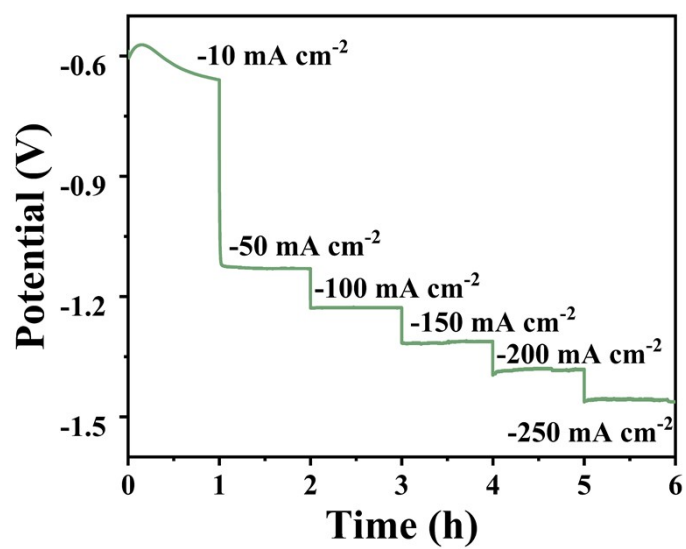


Fig. S9 The multi-step chronopotentiometric curve of the S/NiMoSe.

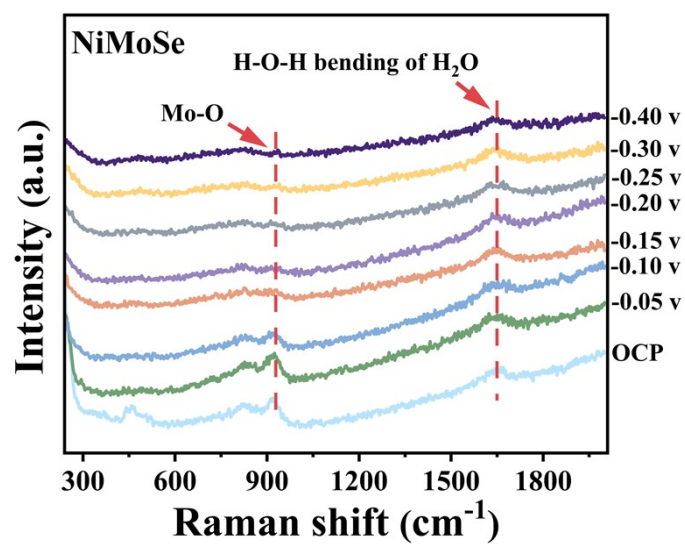


Fig. S10 In-situ Raman spectra of NiMoSe during HER process.

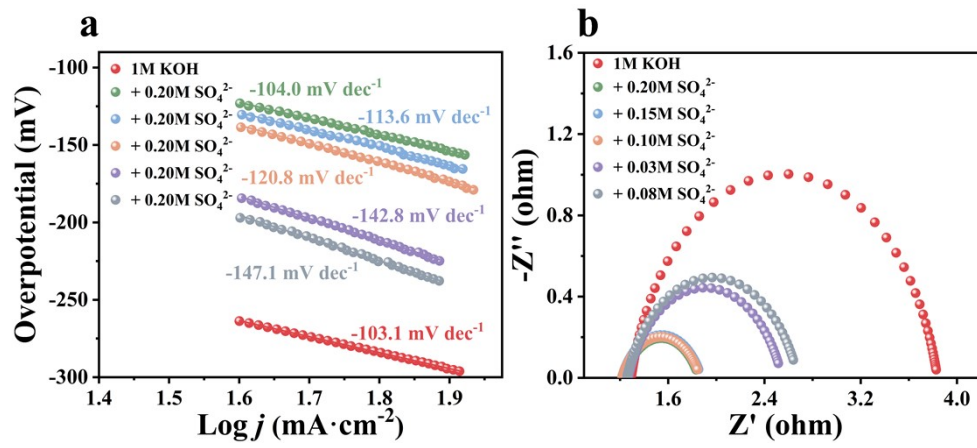


Fig. S11 (a) Tafel slope and (b) EIS Nyquist plots at -1.15eV of NiMoSe in 1M KOH with different concentrations of SO_4^{2-} .

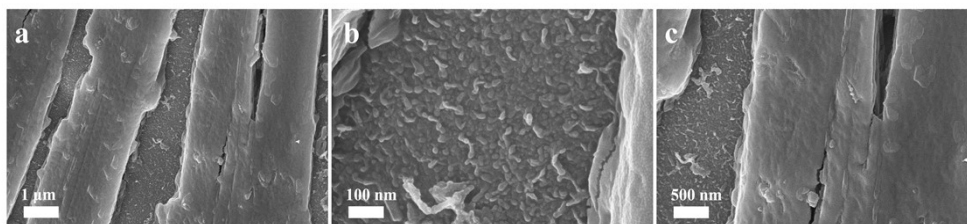


Fig. S12 SEM image of S/NiMoSe after 41 h HER stability test.

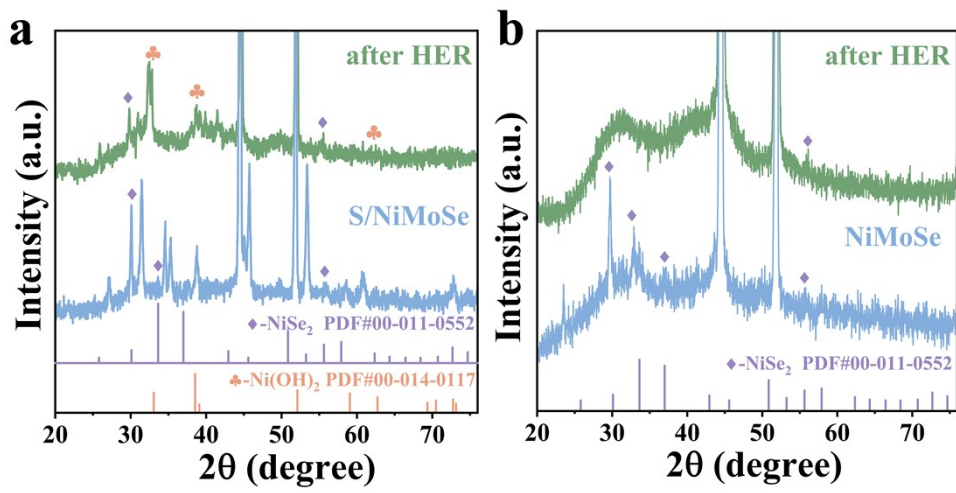


Fig. S13 XRD patterns of (a) S/NiMoSe and (b) NiMoSe before and after HER stability test.

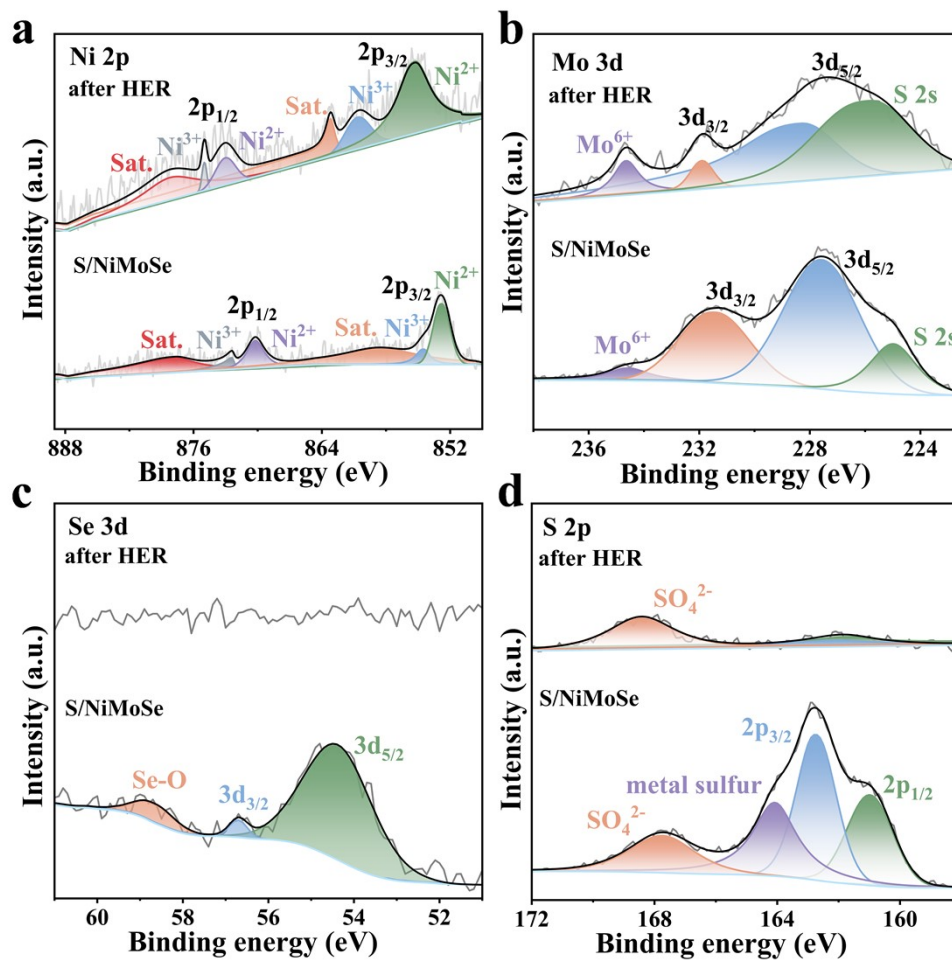


Fig. S14 XPS spectrum of S/NiMoSe after HER stability test (a) Ni 2p, (b) Mo 3d, (c) Se 3d, and (d) S 2p.

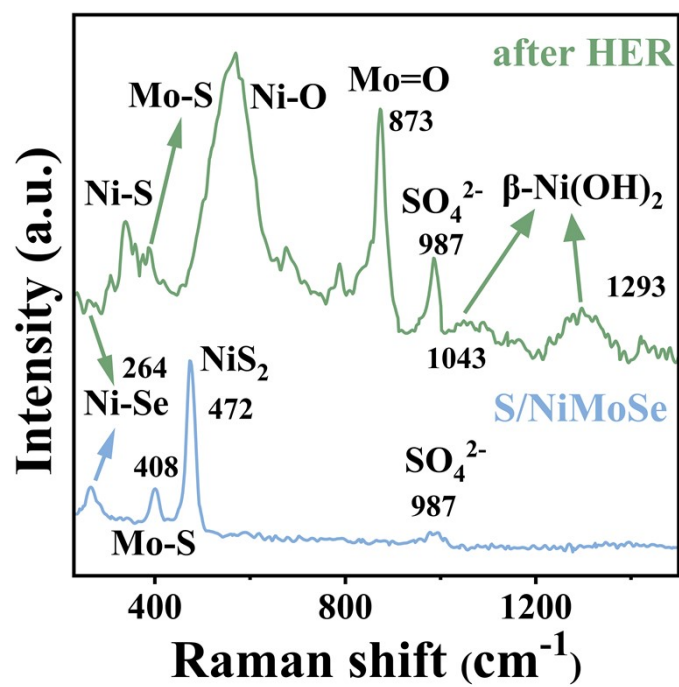


Fig. S15 Raman spectra of S/NiMoSe before and after HER stability test.

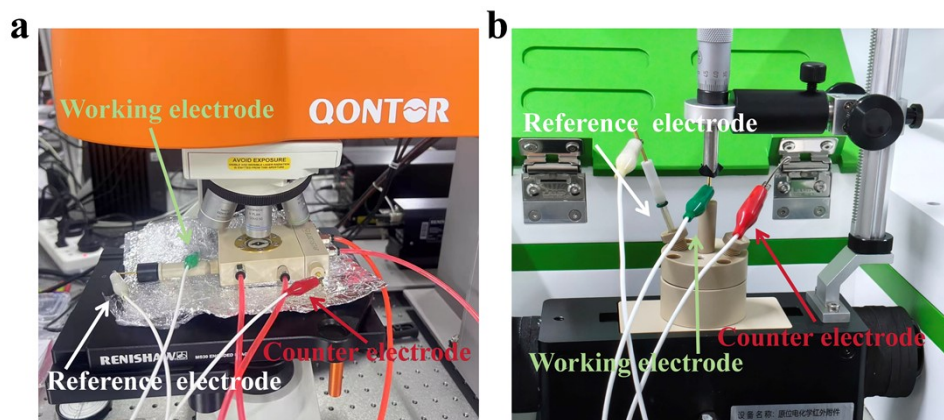


Fig. S16 (a) Photograph of the in situ Raman setup; (b) Photograph of the in situ FTIR setup.